Appl. Phys. B 75, 453–456 (2002)
DOI: 10.1007/s00340-002-0999-0

Applied Physics B
Lasers and Optics

Y.F. CHEN[1,✉]
Y.P. LAN[2]

Spontaneous transverse pattern formation in a microchip laser excited by a doughnut pump profile

[1] Department of Electrophysics, National Chiao Tung University, Hsinchu Taiwan
[2] Institute of Electro-Optical Engineering, National Chiao Tung University, Hsinchu, Taiwan

Received: 20 March 2002/Revised version: 20 May 2002
Published online: 25 October 2002 •

ABSTRACT A transition from a pure Laguerre–Gaussian (LG) mode to a pattern of optical vortex lattices in a large-Fresnel-number microchip laser is experimentally demonstrated by controlling the cavity Q-factor. The cooperative frequency locking of nearly degenerate modes is found to be a primary process for the generation of the optical vortex lattices in a class-B laser. When the cavity Q-factor is high enough, a LG-like mode and a structure of optical vortex lattices are found to coexist. Competition between coexisting transverse patterns of different symmetry gives rise to chaotic fluctuations.

PACS 42.55; 42.65

1 Introduction

Spatio-temporal pattern formations appear spontaneously in a wide range of systems, including hydrodynamics, granular media, chemical reactions and optics, when they are driven sufficiently far from thermodynamic equilibrium [1–4]. In an optical system far from equilibrium, two types of pattern formation have been identified [5]. One is called a pure pattern, which can be successfully described in terms of the empty-cavity eigenmodes, in the absence of non-linearities. Non-linearities imply the interaction of many eigenstates, or pure patterns. The other is essentially non-linear pattern formation that generally requires a large-Fresnel-number resonator.

Depending on the material decay constants and photon decay rate, laser media are roughly classified into three type, Class A, B and C. In a Class A laser, both the material polarization dephasing and population decay rates are much larger than the photon damping rate, and the material variables can be regarded as being slaved to the latter. A Class B laser differs in that the polarization-dephasing rate greatly exceeds the photon and population decay rates, and hence it is slaved to the other two variables. In a Class C laser, all damping rates are comparable in magnitude. The theoretical investigation of non-linear pattern formation is generally based on solving the order parameter equation (OPE). The OPE for a class-A laser is the complex Swift–Hohenberg equation (CSHE) [6–9], whereas the OPE for a class-B laser is a CSHE coupled to the slow population equation [10–12]. The numerical integration of the CSHE shows that non-zero detuning causes excitation of strip patterns in the one-dimensional (1D) space or of vortex lattices in the 2D case. The vortices are extremely interesting because vortex structure appears so widely in nature, in gases, fluids/superfluids, plasmas and even in living things, as in the helix of DNA. It is expected that the laser pattern dynamics and dynamics of other distributed non-linear systems have common features. However, it is difficult experimentally to observe the non-linearity-controlled patterns in laser systems because the requirements comprise both a large resonator Fresnel number and a high level of degeneracy of transverse mode families.

The recent rapid progress of diode-pumped microchip lasers has driven a renaissance of solid-state laser physics research and has led to novel phenomena [13, 14]. The microchip laser can be easily operated in single longitudinal mode more than ten-times above threshold before the second longitudinal mode reaches threshold, because the gain medium has a short absorption depth, which reduces the longitudinal spatial-hole-burning effect [15]. Here, we clearly demonstrate the dependence of transverse pattern formation on the cavity quality factor (Q-factor) in a large-Fresnel-number microchip laser excited by a doughnut pump profile. Upon increasing the cavity Q-factor, the transverse pattern shows a transition from a pure Laguerre–Gaussian (LG) mode to a non-linear pattern of square vortex lattices (SVLs). The stability of the SVL is found to depend mainly on the transverse mode spacing and the pump power. By further increasing the cavity Q-factor, we find the coexistence of transverse patterns of a LG-like mode and a non-linear SVL structure. Competition between coexisting transverse patterns of different symmetry gives rise to chaotic fluctuations.

2 Experimental setup

The experimental cavity we used is analogous to that described in [16]. The system schematic diagram and the pump profile in the laser system are shown in Fig. 1. The gain medium in the experiment was an *a*-cut 2.0 at.% 1-mm-long Nd:YVO_4 microchip crystal. The absorption coefficient of the Nd:YVO_4 crystal was about 6 mm^{-1} at 809 nm. We set

✉ Fax: +886-35/729134, E-mail: yfchen@cc.nctu.edu.tw

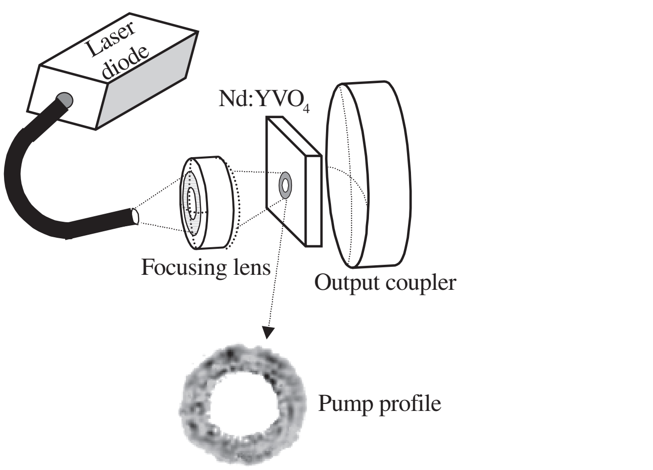

FIGURE 1 Schematic of a fiber-coupled diode end-pumped laser; a typical pump profile of a fiber-coupled laser diode away from the focal plane

up the resonator length to be as short as possible for reaching single-longitudinal-mode operation. The total length in the present resonator was $L = 2.5$ mm. The frequency spacing between consecutive longitudinal modes $\Delta\nu_L$ was about 60 GHz. Since the longitudinal-mode spacing was considerably greater than the transverse-mode spacing, the present laser could be easily operated in single longitudinal mode to study pattern formation. The pump source was a 1-W fiber-coupled laser diode (Coherent, F-81-800C-100) with 100 µm of core diameter. With a special coupling condition, the output intensity of the fiber-coupled laser diode could be controlled to be like a doughnut distribution. The doughnut pump profile was the key technique in the present investigation of pattern formation and competition. The pump power was focused into the microchip gain medium by using a focusing lens with 0.57 magnification.

For a general two-mirror resonator, the Fresnel number can be expressed as $Fr = a^2 / (\pi\omega_o^2)$, where a^2 is the aperture area and $\pi\omega_o^2$ is the area of the lowest-order mode cross. For an end-pumped microchip laser, the effective aperture is usually determined by the pump cross section, not by the mirror aperture. Namely, the Fresnel number for an end-pumped microchip laser is given by $Fr = \omega_p^2 / \omega_o^2$, where ω_p is the pump size of the gain medium. Changing the pump-to-mode size ratio ω_p/ω_o can therefore control the value of Fresnel number. For the present cavity, the mode size of the microchip is given by $\omega_o^2 = \left(\lambda\sqrt{L\ (R-L)}\right)/\pi$, where L is the cavity length and R is the radius of curvature of the output coupler. Three different output couplers were used in the experiment; the radii of curvature were 200 mm, 50 mm and 10 mm. For $L = 2.5$ mm, the mode size of the microchip was calculated to be 0.087 mm, 0.061 mm and 0.038 mm, respectively, for $R = 200$ mm, $R = 50$ mm and $R = 10$ mm. By defocusing the pump source, the pump size could be adjusted within 0.5–0.8 mm. The maximum pump size depended on the lasing threshold. Using $\lambda = 1.064$ µm and $L = 2.5$ mm, the Fresnel number could vary from 35 to 85 for $R = 200$ mm. In contrast, the Fresnel number could vary from 180 to 440 for $R = 10$ mm. Note that the thermal lensing effect was not significant because the thermal power density on the gain medium was controlled to be less than 0.5 W/mm^2.

3 Results

First we used an output coupler of $R = 50$ mm with reflectivity of 97% in the laser resonator. Near lasing threshold, the laser emitted a pure high-order LG $TEM_{0,l}$-mode with the distribution $\cos^2 l\phi$ (or $\sin^2 l\phi$) in azimuthal angle, having $2l$ nodes in azimuth. Laser oscillation on a single high-order LG mode resulted from a doughnut-shape pump profile. As shown in Fig. 2, the free-running single-transverse-mode class-B laser displayed relaxation oscillations, which play an important role in the dynamics of multi-transverse-mode class-B lasers. Slightly above lasing threshold, the present laser usually emitted a pair of transverse LG $TEM_{0,l}$ cosine and sine modes with chaotic dynamics. A non-linear form of the Maxwell–Bloch equation [16] has been used to investigate the interaction of two nearly degenerate transverse modes in a class-B laser. It was found that the appearance of dynamic chaos arises from the interaction of the relaxation frequency and the frequency difference between the nearly degenerate modes. The frequency difference between the nearly degenerate modes generally comes from cross-saturation and other astigmatisms.

The cavity Q-factor is defined as $Q = 2\pi \times$(energy stored)/(energy lost in one oscillation cycle). To excite a continuum of transverse modes simultaneously, we increased the cavity Q-factor by using an output coupler with a higher reflectivity. With an output coupler of $R = 50$ mm with a reflectivity of 99%, we observed a succession of spatially well-organized SVL patterns (Fig. 2), as predicted in [10]. An optical vortex is a point where the field intensity is zero, and the circulation of the phase gradient on any loop which encloses that point is equal to $\pm 2\pi m$ where the integer m is the topological charge of the vortex. As found in [17], the square patterns observed are optical vortices of absolute charge one. The complexity of the SVL pattern increases with the Fresnel number and its axes, along with the orientation of the optical axes of the microchip gain medium. The experimental result confirms the theoretical prediction that the most natural transverse patterns for large-Fresnel-number

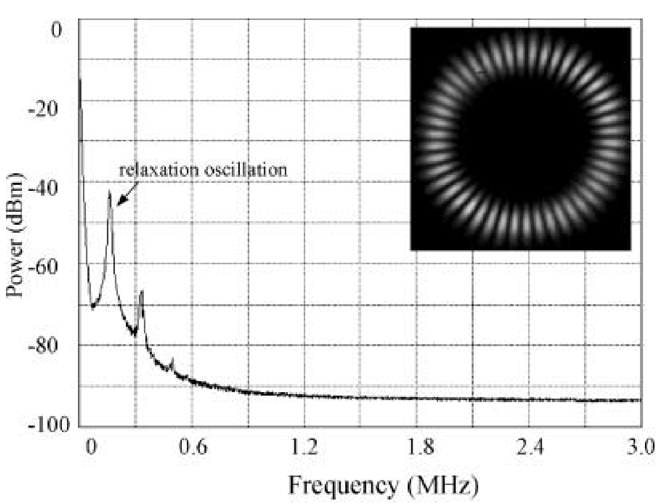

FIGURE 2 Power intensity spectra of laser emission for Laguerre–Gaussian $TEM_{0,23}$ mode near the lasing threshold. The beam profile is shown in the *inset*

lasers are SVLs if transverse-mode families with a high level of degeneracy are excited [6, 10]. Nevertheless, it should be noted that all the analytical investigations deal with plane mirrors, whereas the experimental result presented used curved mirrors. The present experiment also provided the first observation of the transition from linear to essentially non-linear pattern formation in a large-Fresnel-number class-B laser. Measurement of the optical spectrum showed that the SVL pattern was a single-mode emission rather than a combination of multimodes. This result indicates that the formation of SVL patterns is a spontaneous process of transverse mode locking of nearly degenerate modes, assisted by the saturation process of the laser non-linearity. Accompanying the relaxation frequency, the power spectrum of the SVL pattern displays a self-induced oscillation mode, as shown in Fig. 2. The self-induced oscillation mode is generally found to have the same pump-power dependence as the relaxation oscillation. The numerical analysis of the OPEs [10] show that in general it is difficult for a stable SVL pattern to exist in a large-Fresnel-number class-B laser because inertia of population inversion influences the transverse dynamics. Only when the lasing spectrum range is less than the relaxation oscillation frequency can a stable SVL pattern with self-induced oscillations be found in a class-B laser. This situation is consistent with the experimental result that the cooperative frequency locking of nearly degenerate modes is an essential process for finding the self-induced oscillation accompanied by the relaxation oscillation in the SVL pattern. Although similar transverse mode locking in the generation of optical vortex crystals was demonstrated in broad-area VCSELs [17], to date optical systems have not generated such a large number of vortices.

The transverse mode spacing $\Delta\nu_T$ governs the coupling strength between the transverse modes and thus rules the influence of the non-linearity on the dynamical behavior. Theoretical analysis of the OPEs indicates that when the reduced pump parameter ε exceeds the critical value $C\Delta\nu_T/\kappa$, a chaotic regime can appear and the vortices in the square pattern annihilate and nucleate. Here, $\varepsilon = (I_o/I_{th}) - 1$, I_o is the incident intensity, I_{th} is the intensity at the threshold, C is a coefficient of order of unity, and κ is the decay rate of the optical field. To investigate the influence of transverse mode spacing $\Delta\nu_T$, we replaced the output coupler with a $R = 200$ mm concave mirror. The $\Delta\nu_T$ changed from 4.3 GHz to 2.1 GHz at the same cavity length. In this case, the critical pump parameter for the onset of chaos was about $\varepsilon_c = 1.7$. Near the lasing threshold, the dependence of pattern formation on the Fresnel number was almost identical to the previous result, except that a smaller square pattern was emitted due to the larger mode size. When the pump power was increased to $\varepsilon > 2.0$, chaotically moving lattice defects suddenly appear in the SVL pattern and the vortices annihilate and nucleate continuously, as shown in Fig. 4a. A time-series of pictures of the chaotically moving lattice defects is depicted in Fig. 4b. Measurement of the optical spectrum showed that several different transverse-mode frequencies were simultaneously emitted around 1064 nm. The observation of the spatio-temporal instability is in agreement with the theoretical prediction.

By further increasing the cavity Q-factor by using an output coupler of $R = 50$ mm with a reflectivity of 99.9%, a similar SVL pattern was emitted near the pump threshold. For

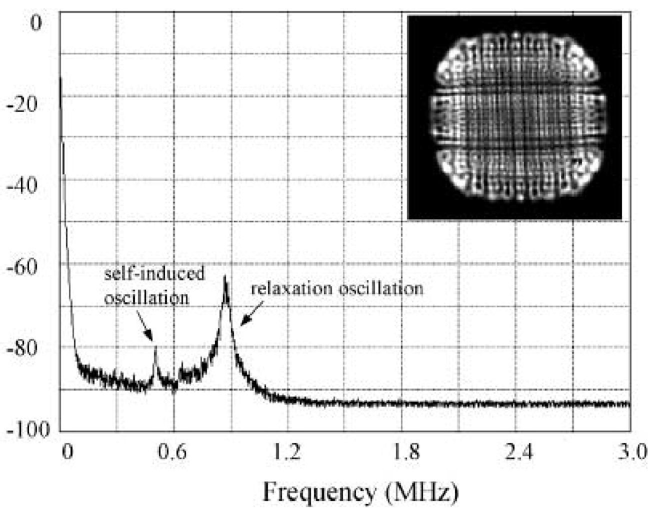

FIGURE 3 Power intensity spectra of laser emission at $Fr \approx 200$, $\varepsilon = 1.0$ and $\Delta\nu_T = 4.3$ GHz. The beam profile of laser emission is shown in the *inset*

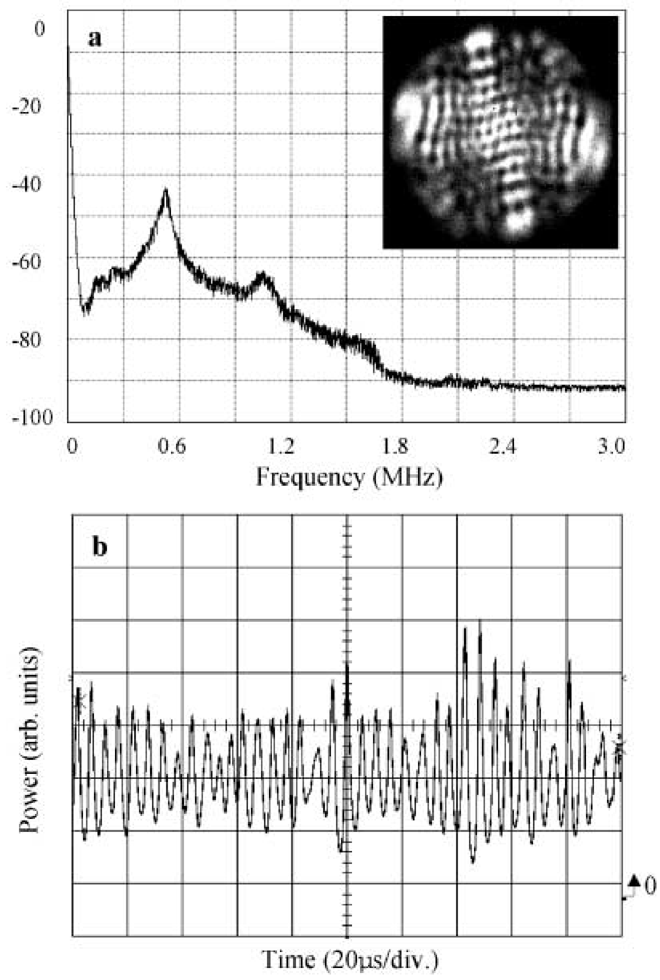

FIGURE 4 **a** Power intensity spectra of laser emission for the square pattern at $Fr \approx 45$, $\varepsilon = 2.1$ and $\Delta\nu_T = 2.1$ GHz. The beam profile is shown in the *inset*. **b** A time-series of pictures of the chaotically moving lattice defects

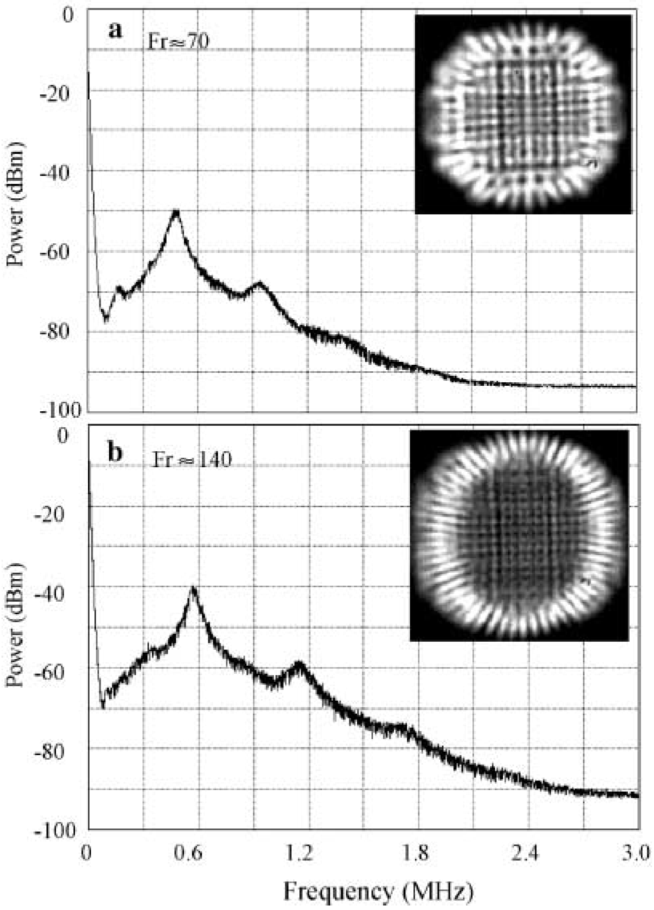

FIGURE 5 Power intensity spectra of laser emission for the square pattern at $\Delta\nu_T = 4.3$ GHz and $\varepsilon = 1.2$: **a** $Fr \approx 70$ and **b** $Fr \approx 140$. The beam profiles are shown in the *insets*

moderate values of the pump parameter power ($1 < \varepsilon < \varepsilon_c$), the transverse mode displayed coexisting transverse patterns that consisted of a LG-like mode on the pump region and a well-organized SVL mode in the center of the boundary, as shown in Fig. 5. The coexistence is understood from the fact that the most natural pattern for minimizing the free energy at the reflecting lateral boundaries is the formation of square vortex lattices; in contrast, the super-high cavity Q-factor with the doughnut-shape pump profile leads to the excitation of a LG-like mode. The first evidence of coexisting patterns of different symmetries was provided in an experiment on parametrically excited surface waves [18]. The different symmetries could be due to either to the selection of different wave vectors corresponding to the same wavelength or to the selection of different wavelengths. The present result belongs to the former case. Recently, the coexistence of domains of different wavelengths has been observed in parametrically excited surface waves [19] and in passive nonlinear optics [20]. In laser systems, this is the first evidence of coexisting transverse patterns of different symmetry. The broadening of the power spectra shown in Fig. 4 indicates that the interaction of two patterns with different symmetries gives rise to time-chaotic fluctuations. The appearance of chaotic oscillations in a coexisting transverse pattern without external periodic perturbations is of considerable interest. The two-mode route to chaotic relaxation oscillations has been observed in a microchip laser with the TEM_{00} mode output in a two-longitudinal-mode oscillation regime [21]. The weak cross-gain coupling among two longitudinal modes has been proposed to explain the relaxation oscillation instabilities. The chaotic oscillation of the coexisting transverse pattern can be explained by the same non-linear gain mechanism.

4 Summary

In summary, we have demonstrated a transition from a pure LG-mode to a pattern of optical vortex lattices in a large-Fresnel-number microchip laser by controlling the cavity Q-factor. Experimental results reveal that the cooperative frequency locking of nearly degenerate modes is an essential process for the formation of stable optical vortex lattices in a class-B laser. The dependence of the SVL dynamics on the transverse-mode spacing agrees very well with the numerical analysis of the order parameter equations. The most striking observation of this investigation is that a super-high cavity Q-factor leads to the coexistence of two transverse patterns with different symmetries and pattern-competition-induced chaotic oscillations.

ACKNOWLEDGEMENTS The authors thank the National Science Council of the Republic of China for financially supporting this research under Contract No. NSC-90-2112-M-009-034.

REFERENCES

1 M.C. Cross, P.C. Hohenberg: Rev. Mod. Phys. **65**, 851 (1993)
2 F. Melo, P. Umbanhowar, H.L. Swinney: Phys. Rev. Lett. **72**, 172 (1994)
3 L.A. Lugiato (Ed.): Chaos, Solitons, Fractals **4**, 1249 (1994)
4 T. Ackemann, W. Lange: Appl. Phys. B **72**, 21 (2001)
5 F.T. Arecchi, S. Boccaletti, P.L. Ramazza, S. Residori: Phys. Rev. Lett. **15**, 2277 (1993); K. Staliunas, G. Slekys, C.O. Weiss: Phys. Rev. Lett. **79**, 2658 (1997)
6 K. Staliunas, C.O. Weiss: Physica D **81**, 79 (1995)
7 J. Lega, J.V. Moloney, A.C. Newell: Phys. Rev. Lett. **73**, 2978 (1994)
8 M. Tlidi, M. Georgiou, P. Mandel: Phys. Rev. A **48**, 4605 (1993)
9 P. Mandel, M. Georgiou, T. Erneux: Phys. Rev. A **47**, 4277 (1993)
10 K. Staliunas, C.O. Weiss: J. Opt. Soc. Am. B **12**, 1142 (1995)
11 J. Lega, J.V. Moloney, A.C. Newell: Physica D **83**, 478 (1995)
12 A. Barsella, C. Lepers, M. Taki, P. Glorieux: J. Opt. B **1**, 64 (1999)
13 M. Möller, B. Forsmann, W. Lange: Chaos, Solitons, Fractals **10**, 825 (1999)
14 K. Otsuka, P. Mandel, E.A. Viktorov: Phys. Rev. A **56**, 3226 (1997)
15 J.J. Zayhowski: IEEE J. Quantum Electron. **QE-26**, 2052 (1990); G.J. Kintz, T. Baer: IEEE J. Quantum Electron. **QE-26**, 1457 (1990)
16 Y.F. Chen, Y.P. Lan, S.C. Wang: Appl. Phys. B **72**, 167 (2001)
17 J. Scheuer, M. Orenstein: Science **285**, 230 (1999)
18 S. Ciliberto, J.P. Gollub: Phys. Rev. Lett. **52**, 922 (1984)
19 B.J. Gluckman, C.B. Arnold, J.P. Gollub: Phys. Rev. E **51**, 1128 (1995); F. Melo, P. Umbanhowar, H.L. Swinney: Phys. Rev. Lett. **75**, 3838 (1995)
20 S. Residori, P.L. Ramazza, E. Pampaloni, S. Boccaletti, F.T. Arecchi: Phys. Rev. Lett. **76**, 1063 (1996)
21 K. Otsuka, S.L. Hwong, B.A. Nguyen: Phys. Rev. A **61**, 3815 (2000)